Author final version

Signatures of rapid trajectory control during finger and arm movements

Niranjan Chakrabhavi [a,b,*], Varadhan SKM [b], Ashitava Ghosal [c,d], Aditya Murthy [a,*]

[a] Centre for Neuroscience, Indian Institute of Science, Bengaluru 560012, India. [b] Department of Applied Mechanics and Biomedical Engineering, Indian Institute of Technology Madras, Chennai 600036, India. [c] Department of Mechanical Engineering, Indian Institute of Science, Bengaluru 560012, India. [d] School of Engineering and Applied Science, Ahmedabad University, Ahmedabad 380009, India. [*] Corresponding Authors – Niranjan Chakrabhavi (niranjanc@iisc.ac.in) and Aditya Murthy (adi@iisc.ac.in).

Abbreviated title: Fast feedback enables rapid trajectory corrections.

First Author: Niranjan Chakrabhavi (ORCID ID: 0000-0003-2583-8689).

Keywords: motor control, trajectory planning, variability, and correlation.

This file includes:

1. Main Text
2. Figures 1 to 8

Supplementary Information (SI): Online Resource is attached with this file containing supplementary methods (SM1 to SM6), results (SR1 to SR3), figures (SF1 to SF2) and tables (ST1 to ST3).

Abstract

Normative goal-directed hand and finger movements often follow invariant kinematics, characterized by approximate straight-line trajectories. A fundamental unresolved issue is whether movement trajectories are planned or whether they are a consequence of trajectory-free online control. We addressed this question using Spearman's rank correlation, zero-crossings rate, and z-scores, and analyzed the time evolution of kinematic variability during the presence or absence of a task in finger and whole-arm reaching movements. We found that the central nervous system (CNS) implements control that is consistent with task-dependent trajectory regulation, where task-relevant movements showed enhanced control toward an average trajectory. Further, we found behavioral signatures of rapid kinematic control that might operate on these planned trajectories as early as ~60 ms in finger movements and ~70 ms in whole-arm reaching movements. Such early signatures of control in behavior suggest that the system could exploit a trajectory plan along with fast feedback to implement meaningful corrections during simple voluntary unperturbed movements. The analysis also revealed that the control peaked distinctly during the early (20%) and late (80-90%) phases, among both finger and arm movements, implying that the extent of trajectory control was not constant during the execution of movement.

Introduction

Normative goal-directed movements are characterized by largely invariant-kinematic patterns consisting of approximate straight-line trajectories that scale with movement amplitude and speed (Morasso 1981), which can be modulated by task demands, and external or biomechanical constraints (Adam 1992; Bohan et al. 2003; Fernandez and Bootsma 2004; Gaveau et al. 2016). Numerous psychophysical and neurophysiological studies further highlight the notion that movement attributes are represented/programmed in the central nervous system well before execution (Keele 1968; Rosenbaum 1985; Dick et al. 1986; Morris et al. 1994; Moran and Schwartz 1999; Padoa-Schioppa et al. 2002; Churchland et al. 2006; Summers and Anson 2009). Such results have motivated the use of internal models, in which a complete specification of a trajectory can, in principle, be made before its implementation (Bizzi et al. 1984; Wolpert et al. 1995; Wolpert and Kawato 1998; Wolpert and Ghahramani 2000; Desmurget and Grafton 2000). However, other influential models of motor control suggest that only certain critical features of the movement such as the target or desired displacement need to be specified in advance (Todorov and Jordan 2002; Desmurget and Grafton 2003; Scott 2004); here, the neural representation specifying movement trajectories may only be generated dynamically in real-time during movement execution as a consequence of solving a cost function based on sensory feedback that is sensitive to the demands of the task. Thus, it remains unclear whether movement attributes, such as trajectories, are planned before execution or derived from trajectory-free online feedback control.Traditionally, online control has been studied in the context of isometric force production tasks (Gordon and Ghez 1987) and reaching movements (Messier and Kalaska 1999; Khan and Franks 2003; Desmurget et al. 2005) where it has been statistically quantified as the lack of predictability of end of task characteristics such as the achieved force, movement amplitude, or movement time from early markers like the peak rate of force, peak velocity or peak acceleration. The method has been validated and further extended by correlating the postures at the end of movement with postures at every time point during the movement (Richardson et al. 2011; Kuang and Gail 2015; Krüger et al. 2017). We used a similar approach to find rapid signatures of online control, based on the premise that planned and derived movement trajectories ought to differ in the timing of their respective control signals that are necessary to mitigate the effects of motor noise, which is a ubiquitous property of muscle and neural activity (Wolpert et al. 2011). More specifically, in the context of planned movement trajectories, a comparison between desired and estimated current states can be used as an error signal to control movements very early, even in the absence of actual sensory information (Gordon and Ghez 1987; Kawato et al. 2003; Richardson et al. 2011). In contrast, derived movement trajectories are expected to rely on delayed sensory feedback to make meaningful corrections during the movement (Todorov and Jordan

2002; Wolpert et al. 2011). Therefore, to isolate rapid online control, we modified previous approaches by correlating postures at the start of movement with those at subsequent time points to identify earlier onsets of trajectory corrections during the movement.

A second feature that could potentially tease apart planned trajectories from trajectory-free control is by investigating the nature of corrections during the movement. Such corrections have been studied in the context of perturbations either to the arm or to the target location (Liu and Todorov 2007; Cluff and Scott 2015), but have not been quantified during normative reaching movements. We developed z-scores and zero crossings rate to estimate the extent of trajectory correction towards a trial-averaged trajectory. The hypothesis was that if the movement trajectories were planned, we would observe such corrections throughout the movement, whereas if the plan consisted only of the target location, these corrections would be concentrated towards the end of the movement.

Using the statistical measures mentioned above, we first demonstrated the presence of rapid kinematic control among the task-relevant instructed fingers and its relative absence among the task-irrelevant non-instructed interdependent fingers during a precise finger flexion-extension task (Chakrabhavi and Skm 2019). We further extended the analysis to investigate simple whole-arm reaching movements.

Materials and Methods

Three experiments with a total of 33 right-handed human participants (experiment-1: cyclic finger flexion-extension, experiment-2: whole-arm reaching, and experiment-3: fast and slow reaching, with 8, 15, and 10 participants respectively, Age: 21-32) were chosen for the study. The experiments were approved by the institute's ethics committees, and participants provided prior informed consent. The Edinburgh Handedness Inventory (Oldfield 1971) was used to evaluate their dominant arm.

Experiment 1: Cyclic flexion-extension movements in fingers

A detailed description of the experiment can be found in Chakrabhavi and SKM (2019). Briefly, the participants sat on a height-adjustable chair and their forearm, palm and thumb finger were secured to the experimental setup, while the index, middle, ring, and little fingers were suspended, and free to move (Fig. 1A).

Finger movements were recorded using electromagnetic tracking sensors (Micro-Sensor 1.8™, 100Hz, Liberty system, Polhemus Inc., VT, USA), attached to the distal phalanges (dorsal side), and the experiment was designed on LabVIEW interface (National Instruments Corp, TX, USA).

The task involved participants to maintain a wrist-posture (0º-neutral, 30º-flexion or 30º-extension) and instructed to perform cyclic flexion-extension movements at the metacarpophalangeal joint with one of the four fingers (index, middle, ring or little) between 75 ± 10 % of maximum flexion-extension limits, and to ignore any involuntary movements in the other non-instructed fingers arising due to finger interdependence/enslavement. Real-time visual feedback of the instructed finger was provided on a screen along with the flexion-extension landmarks, and the half-cycles were timed using an audio metronome (1.5Hz). There were 36 attempts (3 wrist-postures x 4 instructed-fingers x 3 attempts each), and each attempt consisted of 2 seconds of rest followed by 30 seconds of cyclic flexion-extension movements (Fig. 1B). Sufficient practice was provided before the start of the experiment, and movements performed at the neutral wrist posture were considered for the analysis.

Experiment 2: Discrete whole-arm horizontal reaching movements

Participants sat on a backrest supported chair and rested their arm on a smooth elevated table and held onto an endpoint robotic manipulandum (KINARM, BKIN Technologies Ltd., Kingston, Canada) to facilitate horizontal reaching movements (Fig. 1C). Motion of the whole-arm were recorded using electromagnetic tracking sensors (Teardrop Mini sensors, 240Hz, Liberty system, Polhemus Inc., VT, USA), secured over the neck (sternoclavicular joint), shoulder (acromion process), elbow (lateral epicondyle), wrist (dorsal tubercle of radius) and hand (dorsal side), and the motion data from the hand was used for the analysis. Real-time visual feedback of the hand (pink-cursor) was provided on a stimulus screen (LCD, 60 Hz) placed in front of the participant, and the lights were switched off to occlude the vision of the arm. The experiments were executed on TEMPO/VideoSYNC Software (Reflective Computing, MO, USA).

The task required the participants to hold the cursor at the central fixation box for 500 ms, upon which a red colored target appeared in the periphery at any of the eight directions (0º, 45º, 90º, 135º, 180º, 225º, 270º, and 315º, block randomized) at 12 cm eccentricity (Fig. 1D). After a hold time of 1000 ms, the central fixation box disappeared, and they had to make a smooth reaching movement towards the target within 1000 ms (movement time) and stay there for an additional 500 ms to complete the trial, and the success was indicated with an audio

tone. It was ensured that the fixation box and the acceptance window around the target were of the same size. The fixation box then reappeared, and the cursor had to be returned to the center. A minimum inter-trial interval was set to 1500 ms, and the subsequent trial was initiated provided the cursor was within the fixation box. There were approximately ~40 successful trials along each of the eight directions (4 participants performed ~60 trials towards 0º and 45º, and ~20 trials towards other directions). Refer to Online Resource SM1 for an extended description of the central fixation box and successful trials. Practice trials (~10) were provided before the experiment. The task was subsequently performed with the other upper-limb, and the sequence of recruitment was randomized across participants. Movements by the dominant arm have been analyzed and presented here.

Experiment 3: Fast and slow reaching movements

The experiment was designed similarly to experiment-2 with minor modifications. The target color encoded the required speed of movement – green for fast (movement time under 400 ms) and red for slow (movement time between 600-1000 ms), and the conditions were randomly interleaved. This experiment was performed with the dominant arm and towards 0º and 45º directions only.

Data analysis

The data were preprocessed (Online Resource, SM2) and the trials were selected such that the variability between task-relevant and the corresponding task-irrelevant fingers in experiment-1, and of hand positions across task-relevant and the subsequent return movements in experiment-2, were equalized at the movement onset, respectively (Online Resource, SM3, and Fig. SF1A), similar to Gopal et al. (2017).

Online control through trajectory crossovers: Online control was quantified by performing Spearman's rank correlation $\rho(t)$, between the rank order of trajectories at movement onset $R(0)$, with their corresponding rank order $R(t)$, at subsequent time instances $t = 0$ to 100 % (normalized timescale), till the end of movement (Fig. 2A-B, refer Online Resource, SM4). The extent of online control, average decorrelation ($\overline{\rho}$), was quantified by averaging $\rho(t)$ throughout the movement. For arm movements, the $\overline{\rho}$ was further averaged across X and Y coordinates and across all directions of movement. We then fit a logistic function $\rho_f(t)$, over $\rho(t)$ for each subject and used the parameter β to quantify the rate of decrease of $\rho(t)$ using Eq. 1.

$$\rho_f(t) = a + \frac{1}{1 + e^{\beta(\rho(t) - c)}} \quad \textbf{(Eq. 1)}$$

A dispersion (D) measure was computed for the time-normalized trajectories ($A_{n\ x\ T}$ – amplitude matrix) by taking the ratio of average inter-trial standard deviation over the time course (T =101 timestamps between 0 to 100%) with the average range of movement during the *n* trials in Eq. 2. We divided variability by the range to account for differences in movement amplitude, particularly in the finger experiment. We then correlated the average decorrelation ($\overline{\rho}$) with the dispersion measure, expecting that an increased decorrelation leads to lower dispersion.

$$D = \frac{\frac{1}{T}\sum_{j=1}^{T}\sqrt{\frac{\sum_{i=1}^{n}\left(A_{i,j} - \square_j\right)^2}{n-1}}}{\frac{1}{n}\sum_{i=1}^{n}\left|max\left(A_i\right) - min\left(A_i\right)\right|} \quad \textbf{(Eq. 2)}$$

where, $A_{i,j}$ is the amplitude on trial i, at time j, $\square_j$ is the trial-averaged amplitude at time j and A_i is the trajectory on trial i.

Onset of online control: The trajectories were segmented from movement onset to a fixed time instance (300 ms for finger movements and 500 ms for arm movements), and Spearman's rank correlation was performed as described earlier, on this actual time scale. The onset of control was detected, similar to finding the end of the lag phase and beginning of the growth phase in a growth curve, using the 'tangent method' (Bertrand 2019; Smug et al. 2024). A tangent was constructed at the point of maximum rate of decorrelation in the Spearman's correlation coefficient curve, $\rho(t)$, and the initiation of control was identified as the time at which the tangent intersected the ρ = 1 horizontal line.

Constant or time varying online control: Spearman's correlation (ρ_c) was performed as described earlier, but between consecutive 10%-time instances. For example, at *t* = 20 %, correlation analysis was performed between postures at 20 % and 10 % movement duration. If online control were uniform, we would expect ρ_c to be constant,

while if it were time varying, then ρ_c should be a function of time. This analysis was restricted to task-relevant movements.

Quantifying trajectory control with zero-crossings and z-scores: We investigated whether the implemented online control was intended to follow an average trajectory. For any given task, and at every normalized timepoint, each trial was assigned a *z*-score using Eq. 3. Subtraction from the mean was performed to track how the trajectories across different trials moved relative to the average trajectory, and it was normalized by the standard deviation to make it unitless (Fig. 2C-D).

$$z_{i,j} = \frac{A_{i,j} - \mu_j}{\sigma_j} \quad \textbf{(Eq. 3)}$$

where $z_{i,j}$ is the *z*-score of trial i at time j. Parameters μ_j and σ_j are the inter-trial average and standard deviation of the amplitude matrix (A) at time j, respectively.

We quantified trajectory control using the zero-crossings rate (ZCR) as given in Eq. 4, by counting the number of times the trajectories crossed over the average trajectory and dividing it by the total number of trials. This measure was extended to two-dimensional data (ZCR2) in the context of arm movements, where trajectories were produced in a spatial plane (Online Resource, SM5). For arm movements, *ZCR* was averaged across X and Y coordinates, and both *ZCR* and *ZCR2* measures were averaged along all the movement directions. We also computed the measures during the early (0 to 33 %), middle (34 to 66 %), and late (67 to 100 %) phases of movement, to substantiate whether trajectory control was constant or if it varied along the movement. We also analyzed across-trial trends in z-score with respect to the average trajectory (Online Resource, SM6).

$$ZCR\ (\vee\ ZCR2) = \frac{Total\ \ number\ \ of\ \ zero\ \ crossings}{Total\ \ number\ \ of\ \ trials} \quad \textbf{(Eq. 4)}$$

Statistics

The data were checked for normality using the Kolmogorov-Smirnov test. We performed a pairwise t-test for paired comparisons and a two-sample *t*-test for independent comparisons if the data were normal. The Wilcoxon signed rank test, and the Wilcoxon rank-sum test for paired and independent comparisons were used otherwise. For more than two sample paired comparisons, we performed repeated measures ANOVA. Multiple pairwise comparisons were reported with Bonferroni corrections. Mean ± SEM (standard error of mean) was used

to report the statistics unless specified otherwise. Cohen's d was used to report all the effect sizes. A confidence interval (CI) was provided for the timing analysis.

Results

Online control among task-relevant and task-irrelevant finger movements

The differences in the magnitude of online control between the task-relevant and task-irrelevant finger movements were quantified by computing the average decorrelation ($\overline{\rho}$) during the movement (Fig. 3A). A two-way repeated measures ANOVA (4 finger-tasks x 2 finger-type, instructed or non-instructed) showed that the $\overline{\rho}$ of the instructed finger was significantly different from the non-instructed finger ($P < 0.001$, refer to Online Resource, SR1 for extended results, and ST1 for pairwise comparisons).

The dynamics of online control during task-relevant and task-irrelevant finger movements were teased apart by computing the rate of decrease (β) in correlation co-efficient, $\rho(t)$ (Fig. 3A). A two-way repeated measures ANOVA (4 finger-tasks x 2 finger-types, instructed or non-instructed) showed that the rate of decrease of $\rho(t)$ was significantly different between the instructed and non-instructed fingers ($P < 0.001$, refer to Online Resource, SR2 for extended results, and ST2 for pairwise comparisons).

Further, the average decorrelation in finger trajectories was systematically associated with the average trajectory dispersion (Fig. 3B) and was tightly correlated (Spearman's $\rho = 0.9$, $P < 0.001$). The average dispersion of the instructed finger (median = 0.073) was significantly less than that of non-instructed neighboring (median = 0.143, $P < 0.001$) and non-neighboring (median = 0.573, $P < 0.001$) fingers. However, as instructed fingers were associated with varying movement amplitudes, we compared $\rho(t)$ of instructed fingers during all the 4 tasks (instructed index, middle, ring, and little tasks). A one-way repeated measures ANOVA on the task-relevant movements revealed that the $\overline{\rho}$ were not significantly different ($P = 0.72$), and the rate of decrease of $\rho(t)$ were also not significantly different across the instructed fingers ($P = 0.52$), but the range of movement was significantly different between them ($P < 0.001$), with index (10.63 ± 0.27 cm) and the little (7.42 ± 0.27 cm) finger having the highest and lowest movement ranges, respectively.

Next, we quantified the differences in the initiation of control by performing the correlation analysis on the actual timing using the tangent method. We found that the decrease in ρ(t) of the instructed finger (dark purple) was initiated as early as 60.31 ± 1.93 ms (95% CI: [55.76, 64.87] ms). In comparison, decorrelation of the non-instructed neighboring (medium purple) and non-neighboring (light purple) fingers were significantly delayed at 115.25 ± 15.13 ms (P = 0.008, 95% CI: [18.98, 90.91] ms, Cohen's d: 1.28) and 163.64 ± 11.67 ms (P < 0.001, 95% CI: [74.7, 131.95] ms, Cohen's d: 3.02), respectively (Fig. 3C).

Motivated by the previous findings, we examined whether control was constant or occurred during distinct phases along the movement duration. For this, we performed the correlation analysis on the task-relevant finger movements on consecutive 10 % - time instances and found that the controller acted discretely with two prominent troughs in $\rho_c(t)$ at 20th (binomial P < 0.001) and 90th percentile time (binomial P < 0.001) points (Fig. 3D), suggesting the presence of early and late phases of control.

Trajectory control during task -relevant finger movements

We tested the zero-crossings rate (*ZCR*) of the task-relevant and task-irrelevant finger movements during the four different instructed finger tasks to probe the propensity of trajectories to follow an average trajectory (Fig. 4A, and Fig. 2D for the computation method). A two-way repeated measures ANOVA (4 finger-tasks x 2 finger-type, instructed or non-instructed) revealed that the *ZCR* of the instructed finger was significantly different from that of non-instructed fingers (P < 0.001). However, the *ZCR* was significantly different across the 4 finger-tasks (P = 0.025), and interactions between the two factors were significant as well (P = 0.004), indicating that the extent of difference between the instructed and non-instructed fingers depended on which finger was instructed (Refer Online Resource, SR3 for extended results and ST3 for pairwise comparisons).

To support this result further, we divided the initial postures of instructed (solid line) and non-instructed (dashed line) fingers into two groups (Fig. 4B), the ones farther away ($|z|$ > 0.5, purple) and the ones closer ($|z|$ <= 0.5, black) to the average initial posture (z = 0 at percentage time t = 0, movement onset) and found that the away group had a significantly greater propensity to converge towards an average trajectory (0.43 ± 0.02) than the closer ones (0.09 ± 0.02, P < 0.001, Cohen's d: 2.98). Also, the farther away group of the instructed fingers had a significantly greater convergence towards the average trajectory as compared to that in non-instructed

fingers (0.02 ± 0.01, $P < 0.001$, Cohen's d: 5.64). To substantiate the evidence of a temporal structure of control in Fig. 3D, we computed the *ZCR* of task-relevant finger movements across three movement segments (Fig. 4C): early (0 to 33 %, light grey), middle (34 to 66 %, medium grey), and late (67 to 100 %, dark grey) phases of movement duration and found that the *ZCR* was significantly higher during early (0.44 ± 0.01) and late (0.49 ± 0.01) phases as compared to the middle phase (0.27 ± 0.02; Adj. $P < 0.001$ for both the comparisons and Cohen's d: 1.89 and 1.12, respectively).

Online control during whole-arm reaching movements

We investigated whether the correlation analysis performed on finger movements could be extended to whole arm reaching movements and if there were systematic control signatures in the task-relevant movements. We performed the correlation analysis (Fig. 5A) and found that the $\overline{\rho}$ in the task-relevant movements (0.38 ± 0.02) was significantly less than that during fixation (0.98 ± 0.003, $P < 0.001$, Cohen's d: 8.19). A logistic function was fit over $\rho(t)$ (median explained variance = 0.94), to find the rate of decrease (β) in correlation, and it was significantly higher during the task-relevant movements (0.143 ± 0.005) relative to fixation (0.063 ± 0.028, $P < 0.005$, Cohen's d: 0.76). Further, the average decrease in correlation during the task-relevant movements was significantly associated with the corresponding trajectory dispersion (Pearson's $r = 0.57$, $P = 0.02$, Fig. 5B). Further, we estimated that the start of trajectory correction occurred at 69.56 ± 3.45 ms (Fig. 5C, 95% CI: [62.15, 76.97] ms).

Further, to investigate whether online control varied across different phases of movement, we performed the correlation analysis of task-relevant movements on consecutive 10% time instances, $\rho_c(t)$. As was observed in finger movements, we found two distinct troughs at 20th (binomial $P < 0.001$) and around 90th (trough shared between 80th and 90th percentiles, binomial $P < 0.001$ for both time stamps, shared across the participants) percentile time instances, indicating early and late phases of control, respectively (Fig. 5D).

Trajectory control during whole-arm movements

We computed the zero-crossings rate (*ZCR*) for task-relevant movements and compared them with the fixation condition and found that the *ZCR* of task-relevant movements (Fig. 6A, 1.52 ± 0.03) was significantly greater than that during fixation (0.22 ± 0.02; $P < 0.001$, Cohen's d: 10.1). Similar to the analysis in the previous

section, we divided the initial postures (at movement onset) of task-relevant movements into two groups (Fig. 6B), the ones farther away ($|z| > 0.5$, red) and the ones closer ($|z| <= 0.5$, black) to the average initial posture ($z = 0$) and found that the away group had a significantly greater propensity to converge towards an average trajectory (0.57 ± 0.02) than the closer ones (0.12 ± 0.02, $P < 0.001$, Cohen's d: 4.4).

To substantiate the evidence for distinct phases of control, the *ZCR* of task-relevant arm movements was computed across three movement segments (Fig. 6C): early (0 to 33 %, light red), middle (34 to 66 %, medium red), and late (67 to 100 %, dark red) phases of movement duration. We found that the *ZCR* was significantly higher during the early (0.59 ± 0.01) and late (0.53 ± 0.02) phases as compared to the middle phase (0.40 ± 0.01; Adj. $P < 0.001$ for both the comparisons, Cohen's d: 2.56 and 1.93, respectively), similar to that of task-relevant finger movements.

The above zero-crossings analysis was extended to the two-dimensional dataset with trajectories in the XY plane by computing ZCR2 (see methods). The results were qualitatively similar to the one-dimensional analysis. We found that the *ZCR2* of task-relevant movements (red, 1.23 ± 0.04)) was significantly greater than during fixation (grey, Fig. 6D, 0.05 ± 0.01, $P < 0.001$, Cohen's d: 7.97). We further divided the *ZCR2* measure of task-relevant movements into three segments (Fig. 6E): early (0 to 33 %, light red), middle (34 to 66 %, medium red), and late (67 to 100 %, dark red), and found that *ZCR2* during middle phase (0.36 ± 0.02) was significantly less than the early (0.43 ± 0.02, Adj. $P = 0.005$, Cohen's d: 0.87) and late phases (0.44 ± 0.02, Adj. $P < 0.001$, Cohen's d: 1.07).

Differences in control between task-relevant reach movements towards the target and task-irrelevant return movements

As the differences in control measures between fixation and reaches may be related to differences in postural versus movement control, we tested whether these signatures of active control were different across similar movements with varying contexts. For this, we took advantage of the task-irrelevant return movements that were made back to the fixation spot. The maximum inter-trial standard deviation of return movements (1.46 ± 0.05 cm) was significantly greater than the task-relevant movements (1.17 ± 0.05 cm, $P < 0.001$, Fig. 7A). We found that $\overline{\rho}$ in task-relevant movements (Fig. 7B, 0.38 ± 0.02) was significantly less than that of return

movements (0.41 ± 0.01, P = 0.04, Cohen's d: 0.47). This difference in $\overline{\rho}$ was prominent in the first 50 % of the movement duration (task: 0.5 ± 0.02, return: 0.61 ± 0.01, P < 0.001, Cohen's d: 2.02). A logistic function was fit over $\rho(t)$ (median explained variance = 0.97), to find the rate of decrease (β), and it was significantly higher in the task-relevant movements (0.143 ± 0.05) compared to the return movements (0.099 ± 0.006, P < 0.001, Cohen's d: 1.84). Also, the $\overline{\rho}$ during task-relevant movements and the return movements were significantly associated with their respective trajectory dispersion (Pearson's r = 0.53, P = 0.002). Interestingly, the $\overline{\rho}$ during the first 20 % -time duration was significantly less in the task-relevant movements (0.81 ± 0.01) than in the return movements (0.91 ± 0.01, P < 0.001), and it was significantly associated with the respective maximum standard deviation (Fig. 7C, Pearson's r = 0.464, P = 0.009), which interestingly occurred much later during the movement. This association with the maximum standard deviation was maintained even for the duration as early as 10 % into the movement execution (Pearson's r = 0.426, P = 0.018). These differences between task-relevant and return movements were not because of movement kinematics, as the maximum movement speeds were not significantly different across the two conditions (P = 0.62, Online Resource, Fig. SF1B). Further, the maximum rate of change in $\rho(t)$ of the task-relevant movements (128.33 ± 5.62 ms) was significantly earlier than that during return movements (201.38 ± 8.02 ms, P < 0.001, 95% CI: [53.15, 93.96] ms, Cohen's d: 2.03). Using the tangent method, we found that online control during the task-relevant movements was initiated significantly faster than the return movements by 52.58 ± 4.75 ms (Fig. 7D-E, P < 0.001, 95% CI: [42.39, 62.75] ms, Cohen's d: 2.86). We also computed *ZCR2* to find the propensity of the trajectories to follow an average trajectory. We found that the *ZCR2* of task-relevant movements (Fig. 7F, 1.24 ± 0.04) was significantly greater than the return movements (1.16 ± 0.04, P = 0.034, Cohen's d: 0.51). In addition, the farther away group in task-relevant movements (0.57 ± 0.02, Fig. 7G) had significantly greater propensity to converge towards the average trajectory than during return movements (0.33 ± 0.02, P < 0.001, Cohen's d: 2.31).

Invariance of control across different speeds of movement

We subjected the correlation analysis to different movement speeds, between fast and slow conditions (Fig. 8A), to check how sensitive the correlation analysis was to differences in signal-dependent noise, which was expected to be greater for higher movement speeds. As instructed, the maximum speed of fast movements (37.03 ± 0.69 cm/s) was significantly higher than the slow movements (16.58 ± 0.39 cm/s, P < 0.001, Online Resource, Fig. SF1C). Correspondingly, the max SD was higher during fast movements (0.93 ± 0.02 cm) when compared

to the slow condition (0.82 ± 0.03 cm, $P = 0.002$). Nevertheless, we found that $\rho(t)$ for fast and slow movements was largely overlapping and that the $\overline{\rho}$ for fast movements (Fig. 8B, 0.46 ± 0.04) was not significantly different from that of slow movements (0.48 ± 0.05, $P = 0.317$, Cohen's d: 0.33). Further, the average decorrelation was not significantly associated with the max SD across two speeds of movement (Fig. 8C, r = 0.249, $P = 0.289$). Despite that, the rate of decrease in correlation (β) was greater for slower movements (0.130 ± 0.008) when compared to fast movements (0.108 ± 0.005, $P = 0.011$, Cohen's d: 0.88). We also computed the *ZCR2* measure (Fig. 8D) and found no significant differences across fast (0.92 ± 0.08) and slow (1.06 ± 0.12, $P = 0.089$, Cohen's d: 0.60) movements.

Discussion

We used the time course of decorrelation between postures at the initial and subsequent time points to detect rapid online control, the rate of zero crossings around a mean trajectory and the trend of z-scores as signatures consistent with trajectory control, and compared these measures in different contexts of finger and arm movements to show that 1) active online control (or corrections) in trajectories was initiated as early as ~60 ms in task relevant finger movements and ~70 ms in task relevant whole-arm reach movements, providing a framework to identify behavioral kinematic evidence for rapid control during normative unperturbed movements. 2) Such rapid control was compatible with corrections towards an average trajectory. 3) Control was found to be focused over two distinct phases: early (20 %) and late (around 90 %) phases along the time course of finger and arm movements, giving it a w-shaped control structure. 4) Online control was sensitive to the presence or absence of the task but was mostly robust to the range (across instructed fingers) or the speed (across fast and slow) movements.

Identification of rapid online control: in the purview of previous studies

Since Woodworth (1899), a detailed analysis of the kinematics of limb trajectories has provided insights into understanding the relative contributions of motor planning from feedback control (Carlton 1981; Abrams et al. 1990; Chua and Elliott 1993; Abrams and Pratt 1993). In addition to assessing the ability of the motor system to regulate variability throughout the trajectory (Khan et al. 2006), the coefficient of determination (R^2) has been used as a within-trial estimate of the extent to which early kinematic markers (Carlton 1981; Gordon and Ghez 1987; Messier and Kalaska 1999; Desmurget et al. 2005), such as peak acceleration and peak velocity, determine the endpoint distributions. In this context, online control has been inferred by measuring the extent to which such

markers do not predict the endpoint (i.e., lower R^2). Although this approach has been validated by manipulating factors such as the availability of visual feedback (Khan and Franks 2003), the earliest kinematic markers, such as the peak acceleration, happen at ~150 ms, which is too late to reveal fast feedback control. The correlation analysis used in this study implements a similar logic with some important differences that allow us to reveal novel aspects of control during reaching movements. Here, in contrast to previous works that emphasized the relationship of kinematic markers to the end of movement, we measured how quickly trajectories diverged from an initial starting posture, which allowed us to detect corrections to trajectories at the earliest possible time during the movement. To illustrate this, when we performed a preliminary correlation analysis with respect to the end of movement, we did not find significant differences between task-relevant and return conditions during the first 50 % of the arm movements (Online Resource, Fig. SF2), while when the same analysis was performed with respect to the movement onset, the technique was now sensitive to differences in control during this period. Further, the use of Spearman's rank correlation enabled us to attribute crossovers among the trajectories (across trials) as a robust signature of online control and not restrict ourselves to linear associations. We also ensured that the starting variability between different task conditions was not significantly different and that any differences in correlation reflected distinct control structures. Further, the comparison with task-irrelevant movements was particularly useful, since it did not involve manipulation of target locations (Wolpert and Ghahramani 2000; Gritsenko and Kalaska 2010) or postures (Pruszynski et al. 2008, 2011) that would emphasize differences in sensory feedback control as opposed to internally driven control. Finally, and importantly, the absence of any difference in the extent of decorrelation for fast versus slow movements suggests that signal-dependent noise per se was not a factor contributing to the observed decorrelation signal (Fig. 8), however, a relatively smaller yet significant effect was observed in their temporal dynamics (β).

Extent of trajectory control during reaching movements

The demonstration of relatively fast task-related sensory feedback control (~50 ms), which could, in principle, shape trajectories during voluntary movement execution involving active participation of motor cortex (Pruszynski et al. 2011), is a key prediction of trajectory-free optimal feedback control models. However, since movements in optimal feedback models in the absence of trajectory costs are driven by costs associated with the current posture and the target location, they don't necessarily require movements to cross over an average trajectory. This is in contrast with our observations of zero crossings, especially during the early phase, and the trajectories starting farther away had a rapid propensity to converge towards the average $z = 0$ line in the first 20%

of movement duration (Figs. 4 and 6). This suggests the presence of an average planned trajectory computed from the initial fixation to the target location in the exocentric space. Interestingly, this convergence was prominent for the task-related movements as compared to the task-irrelevant movements implying that they were not a consequence of a regression to the mean effect (Fig. 4B, 7F, and 7G). Furthermore, similar zero crossings across different movement speeds (Fig. 8D) suggest that the control is rather robust and is particularly sensitive to the presence or absence of a task.

Further, in contrast to internal models of trajectory control, trajectory-free optimal feedforward/feedback control can also explain straight-line trajectories and is supported by recent work showing the absence of corrective movements to a nominal trajectory in the presence of a perturbation (Cluff and Scott 2015). Although this result cannot be easily reconciled with our results, we suggest that a potential drawback of perturbation studies to assess trajectory control is the assumption that the original normative plan is still relevant during corrections. In the context of target shift experiments, at least, this assumption is questionable as the original plan is expected to be modified or canceled (Mirabella et al. 2008; Murthy et al. 2009). By extension, we assume a similar logic would also hold for external perturbation of the hand. Nevertheless, and interestingly, even in the study by Cluff and Scott (2015), when trajectory specifications such as timing and path were part of the task, corrections were directed to a normative trajectory. In this latter context, our experimental findings broadly agree with them (Cluff and Scott 2015), as our task-relevant finger and arm movements had timing constraints as compared to the corresponding task-irrelevant movements. Additionally, due to the nature of the movements we analysed (cyclic flexion-extension in fingers and centre-out reaches in arm) and our choice of the reference trajectory (the trial-averaged trajectory), trajectory convergence is posited to be towards a task-specific normative trajectory and not necessarily an invariant straight line.

The other important aspect of control we tested is whether the CNS implements a fixed extent of trajectory regulation or if it varies along different phases of movement. Modeling of perturbation studies on arm movements has suggested that the extent of feedback controller gains is lower near movement initiation, while they increase towards the end of the movement as the hand reaches the target (Liu and Todorov 2007). In the context of finger and arm movements, we found that there were two distinct phases of control (Figs. 3D and 5D), which were reflected at time points where there was a relatively large change of decorrelation in the early (trough at 20%) and late (troughs at 80 and 90 %) phases. This was also supported by the relatively greater magnitudes of

zero crossings rate during early and late phases of movement (Figs. 4C, 6C, and 6E). Such a pattern suggests that a trajectory can be efficiently corrected at two extreme postural positions when the velocities of movements are relatively low, and state estimations are more robust. Implementing control close to the target location is obviously beneficial, is synonymous to the homing phase of control, and has been known since the time of Bernstein's seminal experiments (Bongaardt and Meijer 2000), whereas having a high degree of control earlier on has the obvious advantage of clamping variability to manageable levels before the system is swamped by signal-dependent noise (Woodworth 1899; Elliott et al. 2001, 2010). Indeed, we observed that the initial 10 % and 20 % of the decorrelation was predictive of the subsequent trajectory variability (Fig. 7C). However, the relative absence of decorrelation during the middle phase of control suggests that the trajectory control was largely intermittent.

Fast feedback control in normative voluntary movements

Several studies have indicated signatures of relatively fast feedback control involving reflexive arm movements that occur between 50 – 100 ms (in EMG) after the beginning of movements during tasks that require posture/ trajectory stabilization following mechanical perturbations (Messier and Kalaska 1999; Pruszynski et al. 2008, 2011; Nashed et al. 2014; Cluff and Scott 2015). However, whether these feedback signals are also at play during unperturbed normative voluntary goal-directed movements is still not clear. In contrast to such fast sensory feedback, internal feedback control has been shown to implement rapid corrections using an efference copy of the initiated motor command to estimate the hand position via a forward model in the absence of delays associated with sensory feedback (Desmurget and Grafton 2000). To the best of our knowledge, these rapid control strategies have been shown to occur when goals and decisions are changed during movements (Pisella et al. 2000; Gaveau et al. 2003; Desmurget et al. 2005; LoTemplio et al. 2023) to help in fast error corrections. In the context of normative movements, such rapid control has only been studied in the context of fast saccadic eye movements using a similar analysis (Richardson et al. 2011). Evidence of rapid control has also been shown in isometric force application (Gordon and Ghez 1987), but it has not been demonstrated in unperturbed voluntary reaching movements.

In our study, the initiation of control was indexed as the time point of significant decorrelation using the tangent method, and this occurred as early as ~60 ms in voluntary finger movements (Fig. 3C), ~70 ms for voluntary whole-arm reach movements (Figs. 5C and 7D). We interpret this rapid control in reaching movements to be a consequence of internal feedback supplemented with fast sensory feedback processes since the onset of

decorrelation during task-relevant movements occurred less than 50 ms in some subjects performing the reach movement task (two participants in Fig 7E), which is too fast to allow for fast sensory feedback to operate owing to conduction and electromechanical delays (Cavanagh and Komi 1979; Van Acker et al. 2016). However, this rapid onset of decorrelation was typically followed by a later stage that is consistent with fast sensory feedback control, with a maximum rate of decorrelation at ~94 ms for the task-relevant finger and ~128 ms for task-relevant arm movements (Pruszynski et al. 2011; Scott et al. 2015). Such corrections could be mediated by both proprioceptive and visual feedback (Carlton 1981; Saunders and Knill 2003). Additionally, while the rapid trajectory regulation can reflect both feedforward (Elliott et al. 2001, 2010) and feedback processes, we incline towards the latter given the delayed onset of control and the peak decorrelation between 10-20% of the movement phase (Figs. 3D and 5D).

Declarations

Consent to Participate: All the participants provided their written consent for the experiments.

Consent to Publish: All the participants have consented to publication of their anonymized data.

Funding: This research was supported by the Department of Biotechnology – Indian Institute of Science Partnership Program grant (DBT–IISc, *BT/PR27952/INF/22/212/2018*), Intramural funds from IISc (Institute of Eminence grant from the Ministry of Education), and Science and Engineering Research Board grant (SERB, *CRG/2022/000553*). NC was supported by the Prime Minister's Research Fellowship from the Ministry of Education (PMRF, *PM/MHRD-18-16074.03*).

Competing Interests: The authors declare no competing interests.

Ethical Approval: All the experiments discussed in this manuscript have been ethically approved by institute ethics committees at IIT Madras, Chennai, India, and IISc Bengaluru, India.

Data and/or Code Availability: Data for this research article is available upon a reasonable request to the corresponding author.

Author Contribution: NC conceived the study; NC and VSKM designed the finger experiment; NC and AM designed the arm experiment; NC collected data for finger and arm experiment. NC performed the data analysis; AM and AG supervised the analysis; NC and AM wrote the manuscript; NC, AM, AG, and VSKM reviewed the manuscript.

Preprint: A version of this study is available as a preprint on the bioRxiv server – Chakrabhavi N, Vasudevan V, Skm V, Ghosal A, Murthy A (2025) Kinematic signatures of fast feedback trajectory control during goal-directed finger, arm, and saccadic eye movements. :2023.08.09.552575. It is made available under a CC-BY-NC-ND 4.0 International license, at - https://www.biorxiv.org/content/10.1101/2023.08.09.552575v3 .

References

Abrams RA, Meyer DE, Kornblum S (1990) Eye-hand coordination: Oculomotor control in rapid aimed limb movements. Journal of Experimental Psychology: Human Perception and Performance 16:248–267. https://doi.org/10.1037/0096-1523.16.2.248

Abrams RA, Pratt J (1993) Rapid Aimed Limb Movements: Differential Effects of Practice on Component Submovements. Journal of Motor Behavior 25:288–298. https://doi.org/10.1080/00 222 895.1993.9941650

Adam JJ (1992) The effects of objectives and constraints on motor control strategy in reciprocal aiming movements. J Mot Behav 24:173–185. https://doi.org/10.1080/00 222 895.1992.9941613

Bertrand RL (2019) Lag Phase Is a Dynamic, Organized, Adaptive, and Evolvable Period That Prepares Bacteria for Cell Division. Journal of Bacteriology 201:10.1128/jb.00697-18. https://doi.org/10.1128/jb.00697-18

Bizzi E, Accornero N, Chapple W, Hogan N (1984) Posture control and trajectory formation during arm movement. J Neurosci 4:2738–2744. https://doi.org/10.1523/JNEUROSCI.04-11-02 738.1984

Bohan M, Longstaff MG, Van Gemmert AWA, et al (2003) Effects of target height and width on 2D pointing movement duration and kinematics. Motor Control 7:278–289. https://doi.org/10.1123/mcj.7.3.278

Bongaardt R, Meijer OG (2000) Bernstein's Theory of Movement Behavior: Historical Development and Contemporary Relevance. Journal of Motor Behavior 32:57–71. https://doi.org/10.1080/0 022 289 000 9 601 360

Carlton LG (1981) Processing visual feedback information for movement control. Journal of Experimental Psychology: Human Perception and Performance 7:1019–1030. https://doi.org/10.1037/0096-1523.7.5.1019

Cavanagh PR, Komi PV (1979) Electromechanical delay in human skeletal muscle under concentric and eccentric contractions. Europ J Appl Physiol 42:159–163. https://doi.org/10.1007/BF00 431 022

Chakrabhavi N, Skm V (2019) Wrist Posture Does Not Influence Finger Interdependence. J Appl Biomech 35:410–417. https://doi.org/10.1123/jab.2019-0010

Chua R, Elliott D (1993) Visual regulation of manual aiming. Human Movement Science 12:365–401. https://doi.org/10.1016/0167-9457(93)90 026-L

Churchland MM, Santhanam G, Shenoy KV (2006) Preparatory activity in premotor and motor cortex reflects the speed of the upcoming reach. J Neurophysiol 96:3130–3146. https://doi.org/10.1152/jn.00307.2006

Cluff T, Scott SH (2015) Apparent and Actual Trajectory Control Depend on the Behavioral Context in Upper Limb Motor Tasks. J Neurosci 35:12 465–12 476. https://doi.org/10.1523/JNEUROSCI.0902-15.2015

Desmurget M, Grafton S (2000) Forward modeling allows feedback control for fast reaching movements. Trends in Cognitive Sciences 4:423–431. https://doi.org/10.1016/S1364-6613(00)01 537-0

Desmurget M, Grafton S (2003) Feedback or feedforward control: End of a dichotomy. In: Taking action: Cognitive neuroscience perspectives on intentional acts. The MIT Press, Cambridge, MA, US, pp 289–338

Desmurget M, Turner RS, Prablanc C, et al (2005) Updating Target Location at the End of an Orienting Saccade Affects the Characteristics of Simple Point-to-Point Movements. Journal of Experimental Psychology: Human Perception and Performance 31:1510–1536. https://doi.org/10.1037/0096-1523.31.6.1510

Dick JPR, Benecke R, Rothwell JC, et al (1986) Simple and complex movements in a patient with infarction of the right supplementary motor area. Movement Disorders 1:255–266. https://doi.org/10.1002/mds.870010 405

Elliott D, Hansen S, Grierson LEM, et al (2010) Goal-directed aiming: Two components but multiple processes. Psychological Bulletin 136:1023–1044. https://doi.org/10.1037/a0 020 958

Elliott D, Helsen WF, Chua R (2001) A century later: Woodworth's (1899) two-component model of goal-directed aiming. Psychological Bulletin 127:342–357. https://doi.org/10.1037/0033-2909.127.3.342

Fernandez L, Bootsma RJ (2004) Effects of biomechanical and task constraints on the organization of movement in precision aiming. Exp Brain Res 159:458–466. https://doi.org/10.1007/s00 221-004-1964-4

Gaveau J, Berret B, Angelaki DE, Papaxanthis C (2016) Direction-dependent arm kinematics reveal optimal integration of gravity cues. Elife 5:e16 394. https://doi.org/10.7554/eLife.16394

Gaveau V, Martin O, Prablanc C, et al (2003) On-line modification of saccadic eye movements by retinal signals. NeuroReport 14:875

Gopal A, Jana S, Murthy A (2017) Contrasting speed-accuracy tradeoffs for eye and hand movements reveal the optimal nature of saccade kinematics. Journal of Neurophysiology 118:1664–1676. https://doi.org/10.1152/jn.00329.2017

Gordon J, Ghez C (1987) Trajectory control in targeted force impulses. III. Compensatory adjustments for initial errors. Exp Brain Res 67:253–269. https://doi.org/10.1007/BF00 248 547

Gritsenko V, Kalaska JF (2010) Rapid online correction is selectively suppressed during movement with a visuomotor transformation. J Neurophysiol 104:3084–3104. https://doi.org/10.1152/jn.00909.2009

Kawato M, Kuroda T, Imamizu H, et al (2003) Internal forward models in the cerebellum: fMRI study on grip force and load force coupling. In: Progress in Brain Research. Elsevier, pp 171–188

Keele SW (1968) Movement control in skilled motor performance. Psychological Bulletin 70:387–403. https://doi.org/10.1037/h0 026 739

Khan M, Franks I, Elliott D, et al (2006) Inferring online and offline processing of visual feedback in target-directed movements from kinematic data. Neuroscience & Biobehavioral Reviews 30:1106–1121. https://doi.org/10.1016/j.neubiorev.2006.05.002

Khan MA, Franks IM (2003) Online Versus Offline Processing of Visual Feedback in the Production of Component Submovements. Journal of Motor Behavior 35:285–295. https://doi.org/10.1080/0 022 289 030 9 602 141

Krüger M, Straube A, Eggert T (2017) The Propagation of Movement Variability in Time: A Methodological Approach for Discrete Movements with Multiple Degrees of Freedom. Frontiers in Computational Neuroscience 11:

Kuang S, Gail A (2015) When adaptive control fails: Slow recovery of reduced rapid online control during reaching under reversed vision. Vision Research 110:155–165. https://doi.org/10.1016/j.visres.2014.08.021

Liu D, Todorov E (2007) Evidence for the Flexible Sensorimotor Strategies Predicted by Optimal Feedback Control. J Neurosci 27:9354–9368. https://doi.org/10.1523/JNEUROSCI.1110-06.2007

LoTemplio SB, Lopes CL, McDonnell AS, et al (2023) Updating the relationship of the Ne/ERN to task-related behavior: A brief review and suggestions for future research. Frontiers in Human Neuroscience 17:

Messier J, Kalaska JF (1999) Comparison of variability of initial kinematics and endpoints of reaching movements. Exp Brain Res 125:139–152. https://doi.org/10.1007/s002 210 050 669

Mirabella G, Pani P, Ferraina S (2008) Context influences on the preparation and execution of reaching movements. Cognitive Neuropsychology 25:996–1010. https://doi.org/10.1080/0 264 329 080 2 003 216

Moran DW, Schwartz AB (1999) Motor cortical representation of speed and direction during reaching. J Neurophysiol 82:2676–2692. https://doi.org/10.1152/jn.1999.82.5.2676

Morasso P (1981) Spatial control of arm movements. Experimental Brain Research 42:. https://doi.org/10.1007/BF00 236 911

609 Morris ME, Summers JJ, Matyas TA, Iansek R (1994) Current Status of the Motor Program.
610 Physical Therapy 74:738–748. https://doi.org/10.1093/ptj/74.8.738

611 Murthy A, Ray S, Shorter SM, et al (2009) Neural Control of Visual Search by Frontal Eye
612 Field: Effects of Unexpected Target Displacement on Visual Selection and Saccade
613 Preparation. Journal of Neurophysiology 101:2485–2506.
614 https://doi.org/10.1152/jn.90824.2008

615 Nashed JY, Crevecoeur F, Scott SH (2014) Rapid Online Selection between Multiple Motor
616 Plans. J Neurosci 34:1769–1780. https://doi.org/10.1523/JNEUROSCI.3063-13.2014

617 Oldfield RC (1971) The assessment and analysis of handedness: The Edinburgh inventory.
618 Neuropsychologia 9:97–113. https://doi.org/10.1016/0028-3932(71)90 067-4

619 Padoa-Schioppa C, Li C-SR, Bizzi E (2002) Neuronal Correlates of Kinematics-to-Dynamics
620 Transformation in the Supplementary Motor Area. Neuron 36:751–765.
621 https://doi.org/10.1016/S0896-6273(02)01 028-0

622 Pisella L, Gréa H, Tilikete C, et al (2000) An “automatic pilot” for the hand in human
623 posterior parietal cortex: toward reinterpreting optic ataxia. Nat Neurosci 3:729–736.
624 https://doi.org/10.1038/76 694

625 Pruszynski JA, Kurtzer I, Nashed JY, et al (2011) Primary motor cortex underlies multi-joint
626 integration for fast feedback control. Nature 478:387–390.
627 https://doi.org/10.1038/nature10 436

628 Pruszynski JA, Kurtzer I, Scott SH (2008) Rapid Motor Responses Are Appropriately Tuned
629 to the Metrics of a Visuospatial Task. Journal of Neurophysiology 100:224–238.
630 https://doi.org/10.1152/jn.90262.2008

631 Richardson BA, Ratneswaran A, Lyons J, Balasubramaniam R (2011) The time course of
632 online trajectory corrections in memory-guided saccades. Exp Brain Res 212:457–
633 469. https://doi.org/10.1007/s00 221-011-2752-6

634 Rosenbaum DA (1985) Motor Programming: A Review and Scheduling Theory. In: Heuer H,
635 Kleinbeck U, Schmidt K-H (eds) Motor Behavior: Programming, Control, and
636 Acquisition. Springer, Berlin, Heidelberg, pp 1–33

637 Saunders JA, Knill DC (2003) Humans use continuous visual feedback from the hand to
638 control fast reaching movements. Exp Brain Res 152:341–352.
639 https://doi.org/10.1007/s00 221-003-1525-2

640 Scott SH (2004) Optimal feedback control and the neural basis of volitional motor control.
641 Nat Rev Neurosci 5:532–545. https://doi.org/10.1038/nrn1427

642 Scott SH, Cluff T, Lowrey CR, Takei T (2015) Feedback control during voluntary motor
643 actions. Current Opinion in Neurobiology 33:85–94.
644 https://doi.org/10.1016/j.conb.2015.03.006

645 Smug BJ, Opalek M, Necki M, Wloch-Salamon D (2024) Microbial lag calculator: A shiny-
646 based application and an R package for calculating the duration of microbial lag

phase. Methods in Ecology and Evolution 15:301–307. https://doi.org/10.1111/2041-210X.14269

Summers JJ, Anson JG (2009) Current status of the motor program: Revisited. Human Movement Science 28:566–577. https://doi.org/10.1016/j.humov.2009.01.002

Todorov E, Jordan MI (2002) Optimal feedback control as a theory of motor coordination. Nature Neuroscience 5:1226–1235. https://doi.org/10.1038/nn963

Van Acker GM, Luchies CW, Cheney PD (2016) Timing of Cortico-Muscle Transmission During Active Movement. Cereb Cortex 26:3335–3344. https://doi.org/10.1093/cercor/bhv151

Wolpert DM, Diedrichsen J, Flanagan JR (2011) Principles of sensorimotor learning. Nature Reviews Neuroscience 12:739–751. https://doi.org/10.1038/nrn3112

Wolpert DM, Ghahramani Z (2000) Computational principles of movement neuroscience. Nat Neurosci 3:1212–1217. https://doi.org/10.1038/81 497

Wolpert DM, Ghahramani Z, Jordan MI (1995) An internal model for sensorimotor integration. Science 269:1880–1882. https://doi.org/10.1126/science.7569931

Wolpert DM, Kawato M (1998) Multiple paired forward and inverse models for motor control. Neural Netw 11:1317–1329. https://doi.org/10.1016/s0893-6080(98)00 066-5

Woodworth RS (1899) Accuracy of voluntary movement. The Psychological Review: Monograph Supplements 3:i–114. https://doi.org/10.1037/h0 092 992

Figure Captions

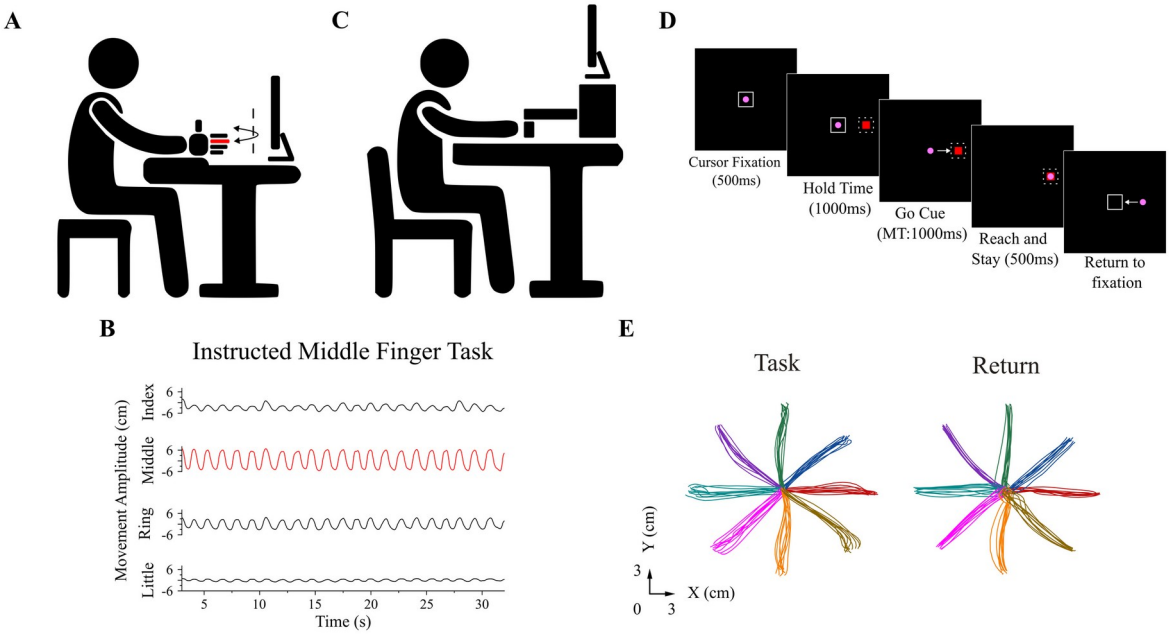
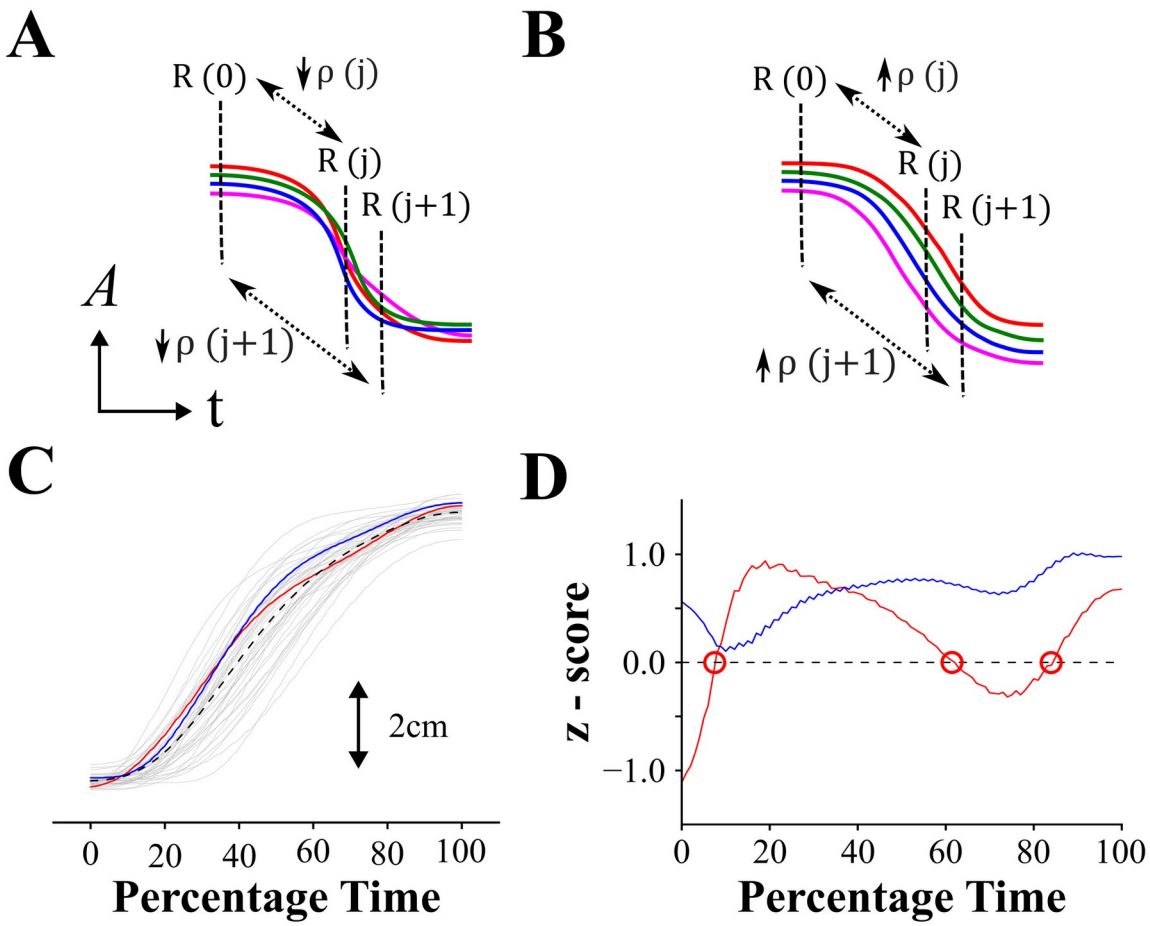


Figure 1: Task design of finger and arm experiments, and their corresponding raw trajectories. *A) Experiment 1: Cyclic finger flexion-extension* – The subjects rested their forearm and palm on a fixed platform in a neutral posture (pronation-supination), the thumb finger was restrained to the setup, and the four fingers (index, middle, ring, and little fingers) were suspended and free to move. On any given trial, the instructed finger (middle finger, depicted with red color, in this case) was instructed to produce cyclic flexion (peaks) and extension (troughs) movements to specified landmarks shown on the stimulus screen (see methods). The phenomenon of finger enslavement led to involuntary movements in the other non-instructed fingers (index, ring and little fingers). *B)* Sample traces of the instructed middle finger task. In this figure, the task-relevant middle finger movement (red color trace) produced task-irrelevant movements in the index, ring, and little fingers. Half-cycles were segmented based on the instructed-finger trace and overlaid against each other for further analysis. *C) Experiment 2: Discrete horizontal whole arm reaching movements* – The experimental setup consisted of a robotic arm that the subject held onto and performed simple reaching movements in the horizontal plane by looking at the stimulus presented on a screen placed in front. *D)* The experimental protocol started with fixating a pink circular cursor in a central fixation box for 500 ms. A red-colored target appeared at an eccentricity of 12cm on the screen. The target location was block randomized to appear at any of the 8 directions (0º, 45º, 90º, 135º, 180º, 225º, 270º, and 315º) with respect to the X-axis. Subjects had to stay at the fixation for 1000 ms during the hold time, and the central fixation box disappeared, marking the go cue to begin the movement. Subjects made simple smooth movements towards the target location within 1000 ms (MT – movement time) and stayed there for an additional

500 ms to complete the trial. The acceptance window around the target location (hollow dashed white square) was the same size as that of the fixation box. They had to then return to the central fixation box for the start of the subsequent trial. *E)* Sample traces of task-relevant movements towards the target and task-irrelevant return movements by the dominant arm of one subject (plotted 10 trials each).



693
694 **<u>Figure 2:</u> Behavioral signatures of online trajectory control.** The colors red, blue, green, and pink in A and B
695 represent four illustrative trials of a given task with a plot of amplitude (A) against time (t). A) If the CNS
696 implements active online control/correction, the rank order at the start of the movement $R(0)$, indicated by red,
697 green, blue, and pink colors from top to bottom, at time $t=0$, is posited to change along the time course and
698 become green, pink, red, and blue ($R(j)$ at time $t=j$), as a consequence of crossovers among the trajectories.
699 These crossovers could be captured as a decrease in the Spearman's correlation coefficient (ρ). By performing
700 the correlation analysis between movement onset and the subsequent time instances $t=0,\ldots j, j+1,\ldots$, we
701 obtain a time varying $\rho(t)$. A low value of ρ indicates greater online control. B) A case where the CNS does not
702 implement online control i.e., the trajectories starting farther away from the average remain farther. The correlation
703 coefficient ρ remains high and closer to 1 along the time course. C) Sample trajectories of the X coordinate of
704 hand movements, directed along 0°, of a single subject, plotted against percentage time. The dashed black line
705 represents the average trajectory, and the red and blue are two selected trials. D) Plot of *z*-scores for the red and
706 blue trials/trajectories and the average trajectory, $z=0$ (dashed black line), as depicted in C. To investigate if the
707 implemented online control was directed towards an average planned trajectory, we computed the number of times

the trajectories crossed the $z = 0$ line for a given set of trials (zero-crossings rate - *ZCR*, see Eq. 4). For example, the red trial has three zero-crossings during the movement (indicated with red circles) and is considered to be under a stronger trajectory control, i.e., a greater propensity towards the average trajectory, while the blue trial had no zero crossings and is said to be under a weaker trajectory control.

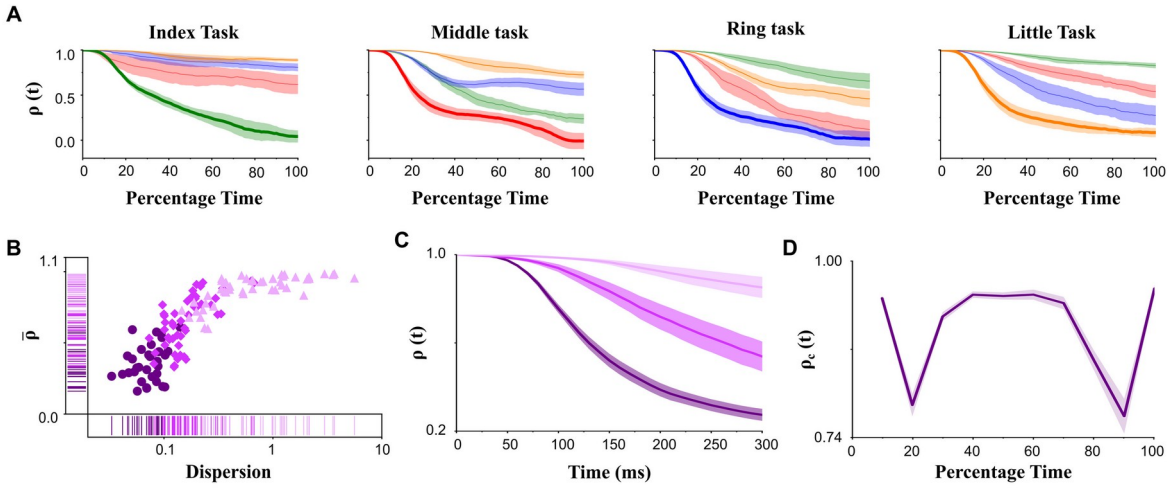
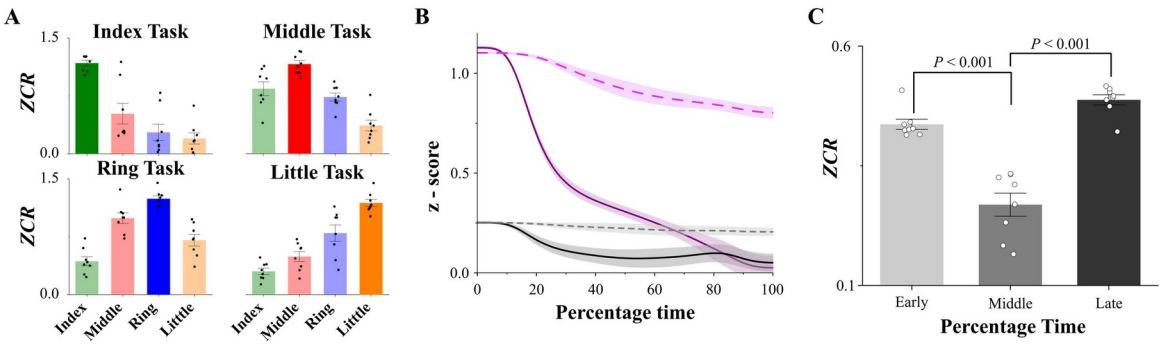


Figure 3: Spearman's correlation analysis of instructed (bold) and non-instructed finger movements. A) The correlation co-efficient, $\rho(t)$, of the four fingers during the instructed index finger task, middle finger task, ring finger task, and the little finger task (mean ± SEM). The decrease in $\rho(t)$ was significantly higher in the instructed finger in all four tasks. Colors: green - index, red - middle, blue - ring, and orange - little fingers. B) Plot of average decorrelation ($\overline{\rho}$) vs trajectory dispersion showed that the instructed fingers (circles) had the lowest $\overline{\rho}$ and lowest dispersion followed by that of non-instructed neighboring fingers (diamonds) and non-neighboring (triangles) fingers. C) The trajectories, $\rho(t)$ (mean ± SEM), of instructed finger, and non-instructed neighboring and non-neighboring fingers plotted from movement onset to 300ms into the movement, and the online control was initiated at 60.31 ± 1.93 ms, 115.25 ± 15.13 ms and 163.64 ± 11.67 ms (mean ± SEM), respectively. D) Correlation analysis of the instructed finger between consecutive 10 % - time instances ($\rho_c(t)$, mean ± SEM). The two distinct phases of control, early control at 20 % and late control at 90 % of movement duration were observed. Colors in Fig. B to D: dark, medium, and light shades of purple represent instructed, and non-instructed neighboring and non-neighboring fingers, respectively.



728
729 **Figure 4: The zero-crossings rate (*ZCR*) of instructed (bold) and non-instructed finger movements and the**
730 **average z-scores.** A) *ZCR* computed from *z*-scores of instructed and non-instructed fingers (mean ± SEM) during
731 index, middle, ring, and little finger tasks. *ZCR* was the highest in the instructed finger of any task (further details
732 in the Results). Colors: green - index, red - middle, blue - ring, and orange - little fingers. B) *z* - scores of instructed
733 (solid line) and non-instructed (dashed line) fingers for trajectories (mean ± SEM) starting away ($|z| > 0.5$, dark
734 and light purple respectively) and closer ($|z| <= 0.5$, black and grey respectively) from the average initial posture
735 ($z = 0$). The trajectories that started farther away from the average trajectory had a greater propensity to come
736 towards the average trajectory ($P < 0.001$), which is a potential signature of trajectory control. This convergence
737 towards the average trajectory was prominent among task-relevant movements compared to task-irrelevant
738 movements ($P < 0.001$). C) *ZCR* of instructed fingers plotted for early (0 to 33 %, light grey), middle (34 to 66 %,
739 medium grey), and late (67 to 100 %, dark grey) movement phases (mean ± SEM). We found that the *ZCR* was
740 significantly greater in the early and late phases as compared to the middle phase (Adj. $P < 0.001$, both cases).
741

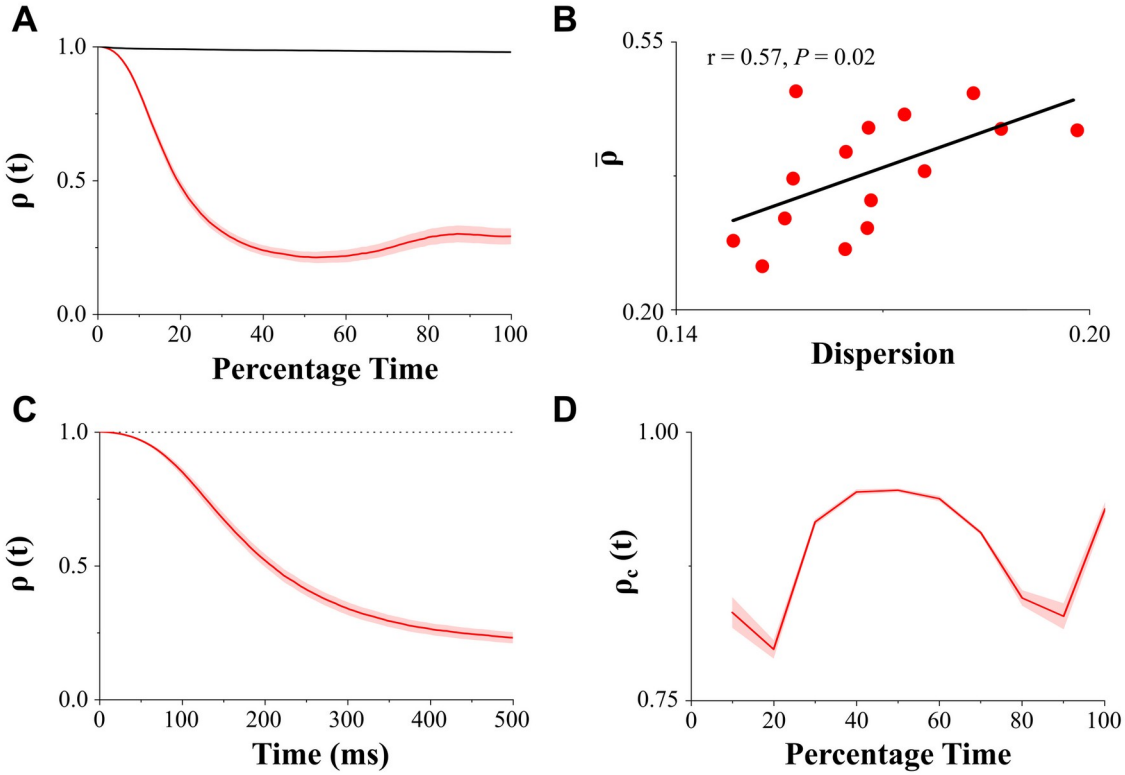


Figure 5: Spearman's correlation analysis of task-relevant arm movements. A) The correlation co-efficient, $\rho(t)$, plotted (mean ± SEM) for task-relevant movements (red) was found to decrease along the movement duration, while it stayed close to 1 during the fixation condition (black). B) The average decorrelation ($\overline{\rho}$) was significantly associated with trajectory dispersion (Pearson's r = 0.57, P = 0.02). A lower correlation value corresponded with a lower trajectory dispersion. C) The correlation co-efficient, $\rho(t)$, plotted on the actual time scale (mean ± SEM) for task-relevant (red) movements. The time at which a tangent line (see methods) from $\rho(t)$ intersected with the $\rho = 1$, dashed black line was at 69.56 ± 3.45 ms (mean ± SEM). D) Correlation analysis of task-relevant movements between consecutive 10 % - time instances ($\rho_c(t)$, mean ± SEM). The two distinct phases of control i.e., early control at the 20th percentile and late control at the 80th and 90th percentile along the movement duration were observed.

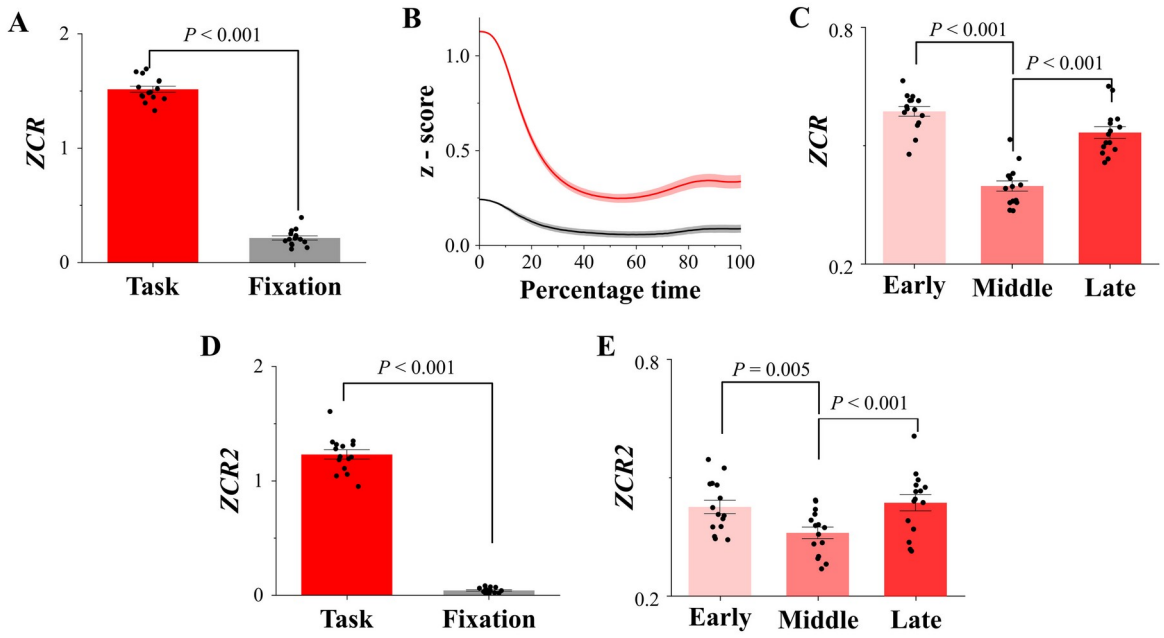


Figure 6: The zero-crossings rate (*ZCR and ZCR2*) and the average z-scores of task-relevant arm movements. A) The 1-dimensional *ZCR* (mean ± SEM) of task-relevant movements (red) was significantly higher than during fixation (black, $P < 0.001$). B) The task-relevant movements were segregated into ones starting farther away ($|z| > 0.5$, red) and closer ($|z| <= 0.5$, black) to the average trajectory ($z = 0$), and we found that the trajectories starting farther away had a greater propensity towards the center than the closer ones (mean ± SEM). C) *ZCR* (mean ± SEM) of task-relevant movements computed at the early (0 to 33 %, light red), middle (34 to 66 %, medium red), and late (67 to 100 %, dark red) movement phases. The *ZCR* was significantly greater during early and late phases as compared to the middle phase of movement (Adj. $P < 0.001$, both cases). D) The 2-dimensional *ZCR2* (mean ± SEM) of task-relevant movements (red) was significantly higher than during fixation (black, $P < 0.001$). E) The *ZCR2* (mean ± SEM) was also significantly greater during the early and late phases, compared to the middle phase (Adj. $P = 0.005$ and Adj. $P < 0.001$, respectively).

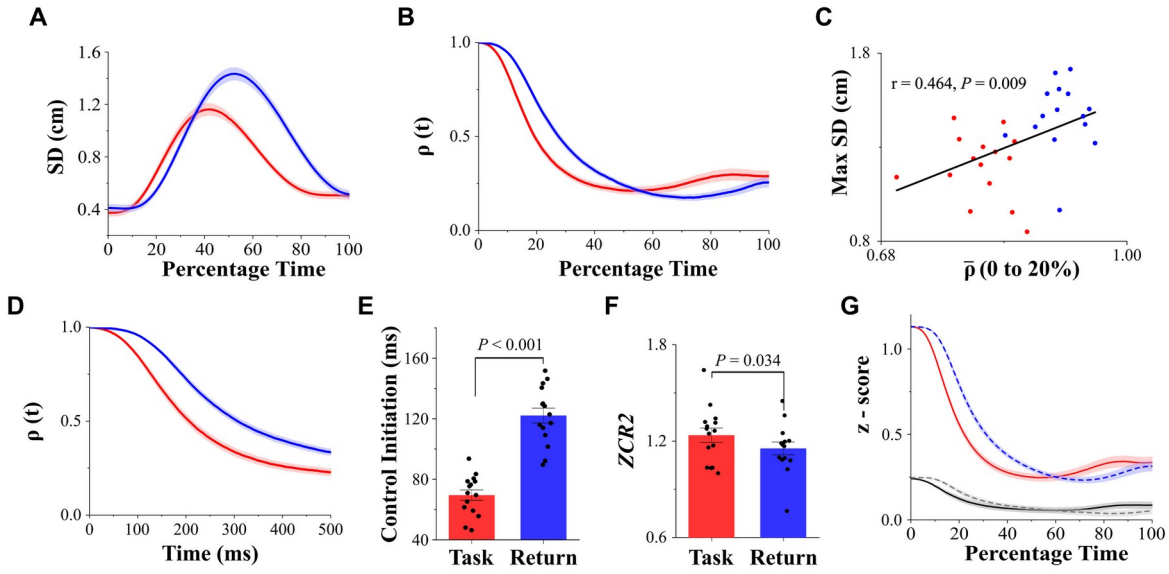


Figure 7: Differences in control between task-relevant (red) vs task-irrelevant return (blue) reach movements. A) The trajectory of inter-trial standard deviation (mean ± SEM) for task-relevant and return movements. Return movements had greater SD than task- relevant movements. B) The correlation co-efficient, $\rho(t)$, of task-relevant and return movements (mean ± SEM). The average decrease in correlation ($\overline{\rho}$) was significantly higher in task-relevant movements (P = 0.04). C) Correlation between $\overline{\rho}$, computed from 0 to 20 % time, with the maximum inter-trial standard deviation of task-relevant and return trajectories. The initial decorrelation among trajectories was significantly associated with the maximum inter-trial variability (r = 0.464, P = 0.009), and the task-relevant movements had lower $\overline{\rho}$ and lesser variability than return movements. D) The variations in correlation co-efficient $\rho(t)$ on the actual time scale from movement onset to 500ms into the movement (mean ± SEM) showed a steeper and earlier decrease for task-relevant movements as compared to return movements. E) The initiation of control marked by the tangent method, showed significantly earlier onset of control during task-relevant movements as compared to return movements by 52.58 ± 4.75 ms (mean ± SEM, P < 0.001). F) *ZCR2* (mean ± SEM) of task-relevant movements were significantly higher than that of return movements (P = 0.034). G) The convergence of z-scores (mean ± SEM) towards the average trajectory in the farther away group was significantly greater among task-relevant movements (solid line, red) as compared to return movements (P < 0.001, dashed line, blue). The solid black line and dashed grey line belong to the closer group of task-relevant and return movements, respectively.

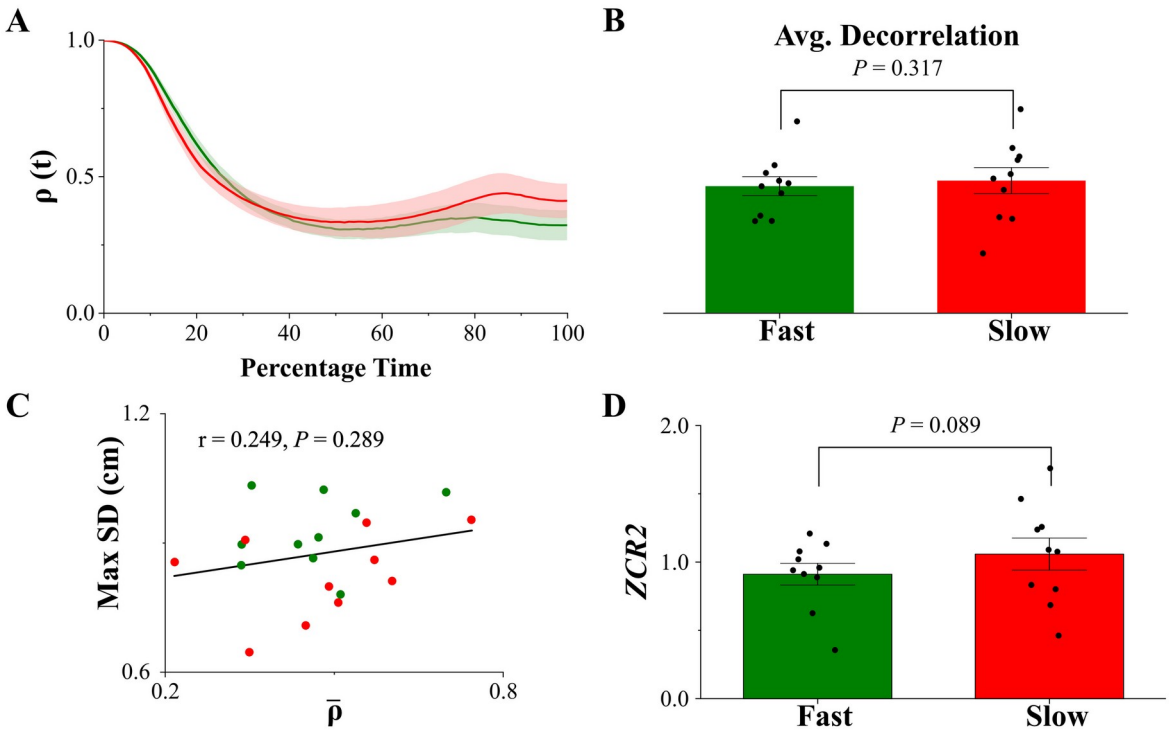


Figure 8: Control analysis on fast and slow reaching movements. A) Plot of co-efficient correlation, $\rho(t)$ (mean ±SEM), of fast (green) and slow (red) movements by the dominant arm. The $\rho(t)$ of fast and slow movements overlapped with each other. B) The average decorrelation ($\overline{\rho}$) was not significantly different between fast and slow movements (P = 0.317). C) The average decorrelation was not significantly associated with the maximum SD (r = 0.249, P = 0.289), even though the maximum SD was higher during fast movements as compared to slow movements (P = 0.002). D) The *ZCR2* was not significantly different between fast and slow movements (P = 0.089).